



24



25 Understanding pathways of recharge to alluvial aquifers is important for maintaining
26 sustainable access to groundwater resources. Water balance modelling is often used to
27 proportion recharge components and guide sustainable groundwater allocations.
28 However, it is not common practice to use hydrochemical evidence to inform and
29 constrain these models. Here we compare geochemical versus water balance model
30 estimates of artesian discharge into an alluvial aquifer, and demonstrate why multi-
31 tracer geochemical analyses should be used as a critical component of water budget
32 assessments. We selected a site in Australia where the Great Artesian Basin (GAB), the
33 largest artesian basin in the world, discharges into the Lower Namoi Alluvium (LNA),
34 an extensively modelled aquifer, to convey the utility of our approach. Water stable
35 isotopes ($\delta^{18}\text{O}$ and $\delta^2\text{H}$) and the concentrations of Na^+ and HCO_3^- suggest a continuum
36 of mixing in the alluvial aquifer between the GAB (artesian component) and surface
37 recharge, whilst isotopic tracers (^3H , ^{14}C and ^{36}Cl) indicate that the alluvial
38 groundwater is a mixture of groundwaters with residence times of < 70 a using ^3H and \sim
39 900 ka using ^{36}Cl methods. In addition, Cl^- concentrations provide a means to calculate
40 a percentage estimate of the artesian contribution to the alluvial groundwater. In some
41 locations, an artesian contribution of up to 70% is evident from the geochemical
42 analyses, contrasting historical water balance modelling estimates of 22%. Our results
43 show that hydrochemical investigations need to be undertaken as part of developing the
44 conceptual framework of a catchment water balance model, as they can improve our
45 understanding of recharge pathways and better constrain artesian discharge to an
46 alluvial aquifer.

47

48



49 **1 Introduction**

50 Recharge to alluvial aquifers can occur via modern infiltration from the land surface and/or
51 discharge into the alluvium from surrounding geological formations and artesian groundwater
52 resources (Costelloe et al. 2012; Schilling et al. 2016; Rawling & Newton 2016; Salameh et
53 al. 2017). Spatial and temporal data resolution and heterogeneity in hydrogeological
54 properties result in considerable uncertainty when allocating recharge to each source and
55 mapping pathways of flow (Anderson & Woessner 1992; Beven 2009; Gardner et al. 2012).
56 Most aquifer systems used in agricultural landscapes have dynamic groundwater gradients
57 due to ongoing groundwater abstraction, which adds to this uncertainty. Flood frequency and
58 intensive pumping from an alluvial aquifer overlying an artesian aquifer (to supply water for
59 irrigated agriculture) can affect head gradients and cause a temporal decrease or increase in
60 artesian discharge and increased mixing. These complexities make it challenging to
61 accurately proportion contributions from various sources to an alluvial aquifer and to guide
62 water allocations. Balancing groundwater allocations is especially difficult when the
63 groundwater is relied upon to sustain ecosystems, the local economy and international export
64 markets.

65 Water balance modelling of aquifers is commonly used to quantify and proportion
66 recharge inputs from river leakage, floodwaters, areal (diffuse recharge) and artesian sources
67 (Anderson & Woessner 1992; Middlemis et al. 2000; Zhang et al. 2002; Dawes et al. 2004;
68 Barnett et al. 2012; Giambastiani et al. 2012; Hocking & Kelly 2016). Historically,
69 hydrochemical analyses are not often used to constrain catchment scale water balance
70 modelling (Reilly and Harbaugh 2004; Barnett et al. 2012). Scanlon et al. (2004) highlighted
71 the need to use multiple techniques (including hydrochemical insights) to increase the
72 reliability of recharge estimates. Geochemical data can improve our understanding of
73 recharge processes because of the potential to trace pathways of groundwater movement and



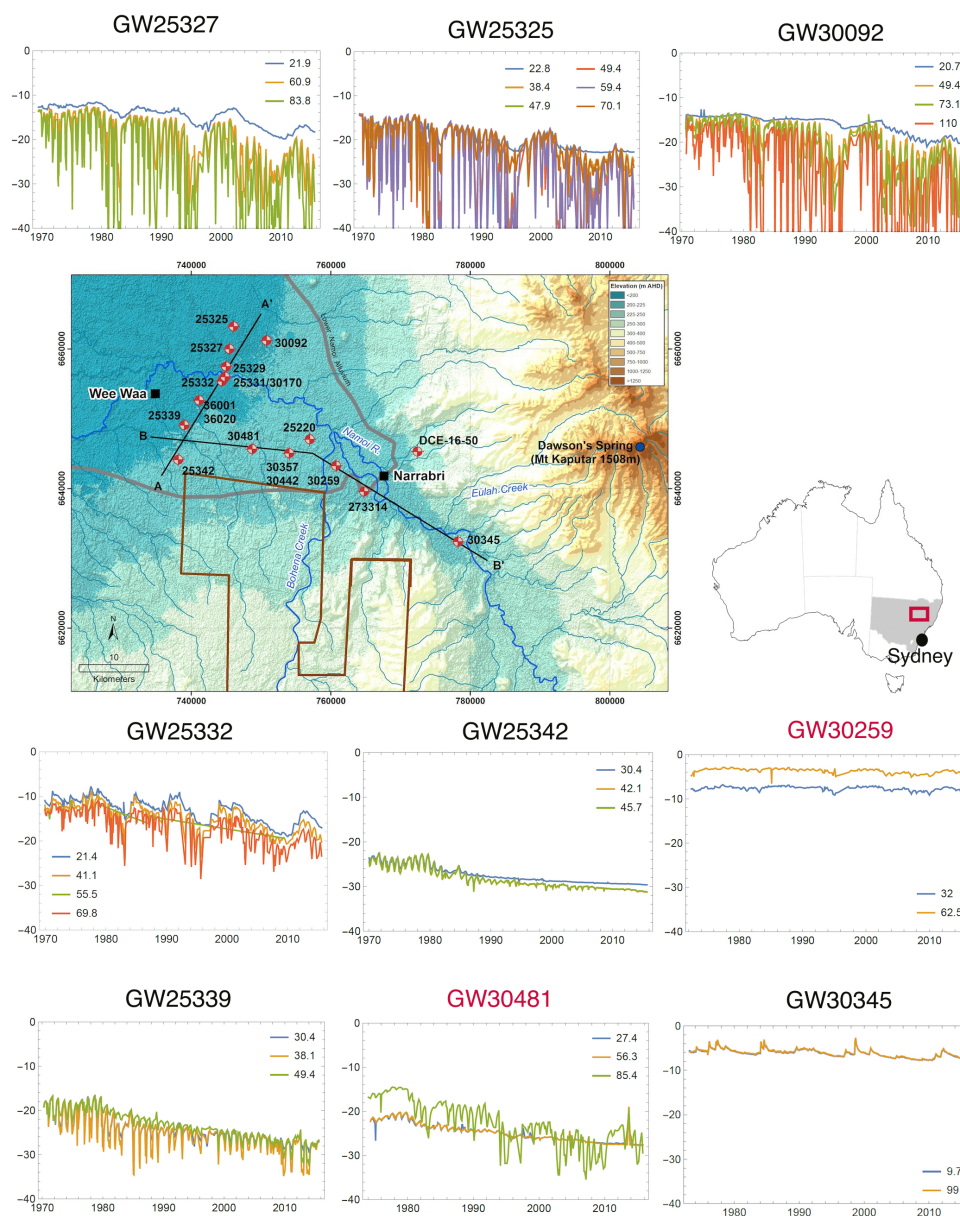
74 water-rock interactions, whilst also providing insights on the impacts of past groundwater
75 extractions (Martinez et al. 2017). Therefore, the integration of geochemical insights to
76 constrain aquifer water balance models provides a more rigorous approach for estimating and
77 proportioning sources of recharge to groundwater resources (Raiber et al. 2015; Currell et al.
78 2017).

79 Radioactive isotopic tracers that provide insights into groundwater residence times can
80 constrain mechanisms of recharge and detect groundwater mixing. However, each tracer has
81 a different half-life, and thus can provide process insights for only a given window of time.
82 Therefore, multiple tracers are needed to cover the time scales relevant for groundwater flow
83 paths. Tritium (^3H) is an excellent indicator of modern recharge inputs in shallow
84 groundwater (Robertson et al. 1989; Chen et al. 2006; Duvert et al. 2016), and provides
85 valuable information on processes active in the past ~ 70 years. Carbon-14 (^{14}C) is used to
86 understand processes active from modern/sub-modern to ~ 30 ka (Clark & Fritz 1997;
87 Cartwright et al. 2010; Cendón et al. 2014) and chlorine-36 (^{36}Cl), whilst applicable in
88 modern groundwater (Tosaki et al. 2007), is usually reserved for the identification of much
89 older groundwater (100 ka to 1 Ma). These isotopes can also trace mixing processes
90 independent of residence time estimations (Bentley et al. 1986; Andrews & Fontes 1993;
91 Love et al. 2000; Moya et al. 2016). Therefore, the combination of ^3H , ^{14}C , and ^{36}Cl dating
92 techniques can provide hydrochemical process insights that cannot be captured by using only
93 one isotope. Identification of recharge and discharge pathways, particularly from underlying
94 artesian contributions, can be better constrained by combining traditional geochemical data
95 with multiple dating techniques and other hydrologic analyses (Amiri et al. 2016; Rawling &
96 Newton 2016; Schilling et al. 2016). We present a multi-tracer approach to constraining
97 artesian discharge from the Great Artesian Basin (GAB) into the Lower Namoi Alluvium
98 (LNA), north-west New South Wales (NSW), Australia (Figure 1). We use water stable



99 isotopes and major ion data to show that recharge to the alluvial aquifer of the LNA is mainly
100 by surface water recharge and artesian inflow from the GAB. We also use ^3H , ^{14}C and ^{36}Cl to
101 show that artesian discharge from the underlying GAB to the LNA is locally much higher
102 than is currently estimated from water balance models used to guide groundwater allocations
103 in the region (Lower Namoi Groundwater 2008). This has implications for ongoing
104 groundwater use in the region, and highlights the need to protect surface recharge zones in
105 both alluvial and artesian portions of catchments.

106 The over-reliance of water balance models used to allocate groundwater resources that
107 have not been constrained by isotopic tracer residence times or hydrochemical results is a
108 common issue globally. This research highlights that comprehensive hydrochemical
109 investigations improve our conceptual understanding of recharge pathways and that such
110 investigations should be applied to all important groundwater resource assessments to enable
111 sustainable management.



112

113 **Figure 1.** Map of the study area and sample locations, along with the location of the study area in
 114 Australia. Accompanying hydrographs show the groundwater level response in different piezometers
 115 throughout the study area (groundwater level data sourced from BOM 2017). The different colours in
 116 the hydrographs represent the different monitoring bores in the nested set. The bottom of the slotted



interval for each bore is shown in the key. The x-axis in each hydrograph is the year (1970-2010) and the y-axis is depth (between 0 and 40 m bgs). The two locations with red text highlight areas where the hydrograph heads show clear GAB contribution. The remaining locations show no apparent GAB contribution to the LNA based on the hydrograph data.

121

122 **2 Study Area**

The lower Namoi River catchment is located in the north-west of NSW, Australia (Figure 1). Groundwater resources in the LNA are the most intensively developed in NSW (DPI Water 2017). For this reason, there is concern regarding groundwater exploitation and threat to the long-term sustainability of the system (Lower Namoi Groundwater 2008; DPI Water 2017). Groundwater abstraction from the LNA supports a multibillion-dollar agricultural sector (focused around cotton growing established in the 1960s), supplying around 50% of water for irrigation in the region (Powell et al. 2011). The first high-volume irrigation bore was installed in 1966 (Rural Forum 1967) and the use of groundwater expanded rapidly throughout the region throughout the 1960s to 1990s. Peak extraction of approximately 170,000 mega litres (ML) occurred over the 1994/1995 growing season (Smithson 2009). Consistently declining groundwater levels and concern regarding the long-term sustainability of groundwater abstraction led to the implementation of a Water Sharing Plan in 2006, which systematically reduced groundwater allocations to the irrigation sector over a ten-year period. The present allocation is 86,000 ML/a (Lower Namoi Groundwater 2008).

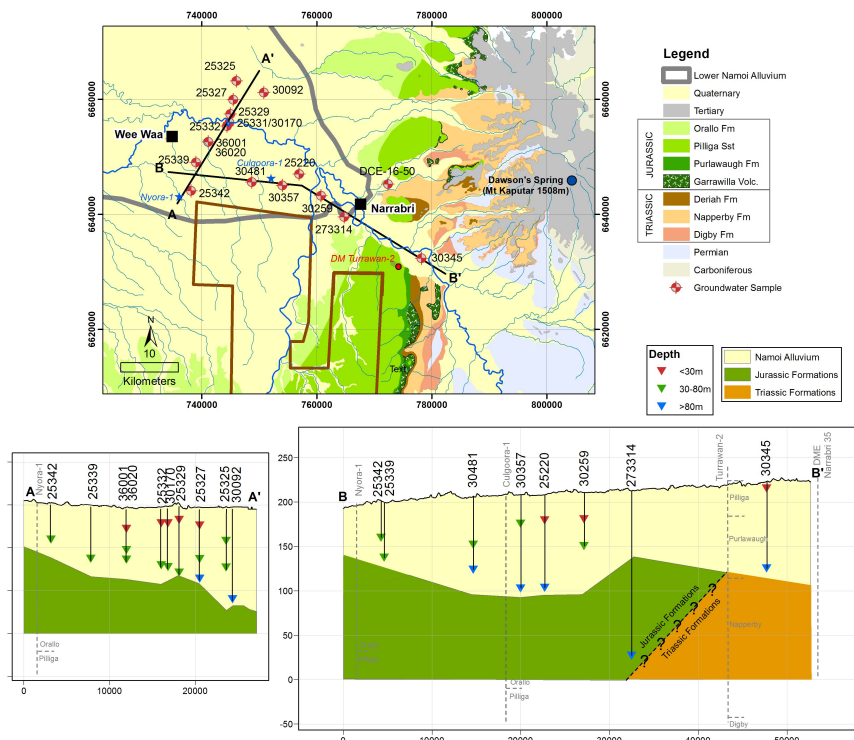
137

138 **2.1 Hydrogeological setting**

The lower Namoi River catchment lies within the Murray-Darling Basin and overlies the confined Coonamble Embayment, which is a subdivision of the Surat Basin, which in turn is a sub-basin of the GAB. The southernmost portion of the LNA is underlain by Triassic formations, while northwest of monitoring bore 30345 the LNA is underlain by Jurassic



143 formations (Figure 2). Within the region of study, the oldest outcropping bedrock formation
144 is the Digby Formation (lithic and quartz conglomerates, sandstones and minor finer grained
145 sediments) (Tadros 1993). The Digby Formation outcrops in the south-east of the area and
146 the Namoi River abuts the formation just south of B' on Figure 2. The Digby Formation is
147 overlain by the Napperby Formation (thinly bedded claystone, siltstones and sandstone). This
148 formation occurs at a depth of 106 m, just below the base of monitoring bore 30345 (NSW
149 Pinneena Groundwater Database, driller logs), where the paleo-Namoi river carved a path
150 through a syncline. In outcrops to the east of the study area, the Napperby Formation is
151 overlain by the Deriah Formation (green lithic sandstone rich in volcanic fragments and mud
152 clasts) (Tadros 1993), however this has not been identified beneath the bores used in this
153 study. The boundary between the Triassic and Jurassic lies west of monitoring bore 30345.
154 There is an unconformable boundary between the Triassic and Jurassic formations, and in
155 some outcropping regions the Garrawilla Volcanics (alkali basalts, trachyte, hawaite,
156 pyroclastic and subordinate sediments) is the base Jurassic formation. Overlying the
157 Garrawilla Volcanics are the Purlawaugh Formation (carbonaceous claystone, siltstone,
158 sandstone and subordinate coal), Pilliga Sandstone (medium to coarse quartzose sandstone;
159 Tadros 1993) and the Orallo Formation (clayey to quartzose sandstone, subordinate siltstone
160 and conglomerate) (Tadros 1993). The Pilliga Sandstone forms the bedrock below
161 monitoring bores 25325 to 25342, and in the Namoi region is the primary aquifer of the
162 GAB.



163

164 **Figure 2.** Two cross sections through the study area, showing the location and depth of the samples in
 165 the alluvium and their proximity to formations of the GAB. Contacts obtained from gas wells Nyora-
 166 1, Culgoora-1 and Turrawan-2, coinciding with our cross sections, are added. Their locations are
 167 displayed on the map.

168

169 From the late Cretaceous to the mid Miocene, a palaeovalley was carved through the
 170 basement rocks (Kelly et al. 2014). Then from the mid Miocene until present, the palaeovalley
 171 was filled with reworked alluvial sediments. Groundwater abstraction in the study area is
 172 mostly from these alluvial sediments. Fluvial and aeolian interbedded clays, silts, sands and
 173 gravels form the up to ~ 140 m thick alluvial sequence of the Lower Namoi Catchment
 174 (Williams et al. 1989). Traditionally, three main non-formally defined aquifers/formations have
 175 been used to describe the LNA. The semi-confined Cubbaroo Formation overlies the bedrock in



176 the northern palaeochannel (which passes beneath monitoring bores 25325 and 30092). This
177 formation is up to 60 m thick. The Cubbaroo Formation is overlain by the semi-confined
178 Gunnedah Formation, which is up to 80 m thick, and is conformably overlain by the unconfined
179 Narrabri Formation, which is 10 to 40 m thick (Williams et al. 1989). However, more recent
180 research in the Namoi Catchment suggests that the rigid subdivision in to the Narrabri,
181 Gunnedah, and Cubbaroo formations or aquifers based on depth (upper, middle, lower) cannot
182 easily explain the continuum in chemical evolution observed (discussed further below) or the
183 facies distribution (Kelly et al. 2014, Acworth et al. 2015). Kelly et al. (2014) argue that the
184 sedimentary sequence is better represented as a distributive fluvial system, with high energy
185 sedimentary gravel and sand deposits dominating at depth and low energy silt and clay
186 deposition dominating near the ground surface. This is due to a shift from a relatively wet
187 climate in the mid Miocene (greater than 1500 mm annual rainfall; Martin 2006) to the present
188 drier climate in the region, which averages approximately 660 mm at Narrabri (BOM). There
189 is also a higher proportion of gravel and sand deposits in the proximal portion of the catchment,
190 between Narrabri and Wee Waa (the area of this study), than the distal portion of the system
191 west of Cryon (Kelly et al. 2014). Acworth et al. (2015) showed that within the alluvial
192 sequence there are time gaps of hundreds of thousands to millions of years in the sedimentary
193 sequence, which is expected in meandering river sedimentary environments.

194

195 **2.2 Current understanding of recharge and discharge processes in the Lower Namoi**

196 **Alluvium**

197 There have been many investigations in the study area because of the local and national
198 economic importance of the LNA. These investigations encompassed both catchment water
199 balance models and hydrochemical investigations. However, the hydrochemistry of the



200 groundwater in the region has not been used in conjunction with water balance modelling
201 prior to this study (Merrick 2001; CSIRO 2007; Kelly et al. 2007).

202

203 2.2.1 Water balance modelling of recharge

204 To guide groundwater allocations from the LNA, a series of water budget models were
205 developed using MODFLOW (Merrick 1989, 1998a, 1998b, 1998c; 1999, 2000; 2001). The
206 complete history of the development of these models is discussed in Kelly et al. (2007).
207 These models were driven by climatic, rainfall, flood and streamflow data and calibrated to
208 groundwater head data. There are equivalent solutions for all water balance models and the
209 solution presented is often constrained by several factors. These constraining factors include
210 geological insights; the modeller's experience and biases, for example, the way diffuse
211 recharge is modelled either as a percentage of rainfall (Merrick 2001; CSIRO 2007) or as a
212 complex evapotranspiration function (Giambastiani et al. 2012); verification measures and
213 pragmatic goals. One MODFLOW derived water balance model presented in Merrick (2001)
214 proportioned the recharge for the water budget period 1980-1994 as following: flood and
215 diffuse rain recharge 24,100 ML/a, stream recharge 33,700 ML/a, up gradient alluvial inflow
216 3,060 ML/a, and artesian (GAB) recharge 9,500 ML/a. In that model, artesian recharge was
217 inferred to primarily occur in the eastern portion of the model (between Narrabri and Wee
218 Waa), which overlaps with this study area (Figure 1). The zone between Narrabri and Wee
219 Waa accounted for 42,700 ML/a of the total recharge to the LNA. Thus, according to the
220 model the artesian discharge into the LNA in this area equated to 22%. When the LNA
221 MODFLOW model was calibrated there was no consideration given to using hydrochemical
222 data to constrain the calibration (Merrick 2001; CSIRO 2007; Kelly et al. 2007).

223

224



225 2.2.2 *Hydrochemical estimates of recharge*

226 The first isotopic investigation in the area was conducted from 1968 to 1975 and partially
227 published by Calf (1978). The author used ^{14}C and ^3H to assess recharge pathways to the
228 LNA and found evidence for river recharge in the upper aquifer, and that modern
229 groundwater penetrated the deeper parts of the LNA. Calf (1978) also found evidence for
230 ‘leakage’ of groundwater from the GAB up into the deeper LNA, however volumetric
231 estimates were not provided.

232 McLean (2003) conducted an extensive hydrochemical and isotopic characterisation of
233 both the GAB groundwater and the alluvial groundwater in 1999-2000. This research
234 concluded that mixing of groundwater from the GAB into the lower and middle parts of the
235 LNA is an important process especially in the south of the catchment. This study also did not
236 quantify the amount of mixing occurring between the two groundwater sources.

237

238 **3 Materials and methods**

239 **3.1 Groundwater collection**

240 This study comprised two field campaigns, the first one from 28 January 2016 to 8 February
241 2016 (summer) when the aquifer was stressed by pumping for irrigation, and the second from
242 21 June 2016 to 30 June 2016 (winter) in the absence of abstraction for irrigation.

243 In summer, we collected groundwater samples from 28 NSW Department of Primary
244 Industries Water (DPI Water) monitoring bores and a surface water sample from the Namoi
245 River. In winter, we collected groundwater samples from 16 NSW DPI Water monitoring bores
246 and surface water samples from the Namoi River and 2 upstream tributaries (see
247 Supplementary Table 2 for locations). The bores are screened at varying intervals, intersecting
248 the shallow, middle and deep alluvium. Most bores were sampled with either a Grundfos (MP1
249 sampling pump) or Bennett compress air piston pump, with the pump placed ~ 1 m above the



250 screen when using the Grundfos pump and a drop-tube extension adjusted to place the pump
251 intake within the screen when using the Bennett pump. Some deep monitoring bores were
252 sampled with a portable bladder pump using low-flow methods (Puls & Barcelona, 1996). In
253 these bores the pump was placed approximately 10 m below standing water level, with a drop-
254 tube cut to place the pump intake within the screen. For shallower bores (less than 50 m), a 12
255 V battery operated pump was used with the pump intake placed ~1 m above the screen. For all
256 sample sites, physico-chemical parameters (pH, DO, EC) were monitored and samples
257 collected once three well volumes had been pumped and/or the physico-chemical parameters
258 stabilised. This was generally achieved within 1 to 3 hours after onset of pumping. Sample
259 collection involved an in-line, 0.45 μm , high-volume filter connected to a high density
260 polyethylene (HDPE) tube. Total alkalinity concentrations (field alkalinity) were determined in
261 the field by acid titration using a HACH digital titrator and external pH meter control. The Fe^{2+}
262 and HS^- concentrations were determined using a portable colorimeter (HACH DR/890).

263 Samples for anion and water stable isotope ($\delta^2\text{H}$ and $\delta^{18}\text{O}$) analyses were collected in 60
264 mL and 30 mL HDPE bottles, respectively, with no further treatment. Samples for cation
265 analysis were collected in 60 mL HDPE bottles and acidified with ultrapure nitric acid.
266 Samples for ^{14}C and ^3H were collected in 1 L narrow mouth HDPE bottles and 2 L HDPE
267 bottles respectively, and were sealed with tape to avoid potential atmospheric exchange during
268 storage. Samples for ^{36}Cl were collected in 1 L narrow mouth HDPE bottles with no further
269 treatment. Major ion and ^{14}C samples were refrigerated at 4°C until analysed.

270 For both sampling campaigns, we aimed to collect samples representative of the river,
271 the alluvium and the GAB, however we were not able to access any previously characterised
272 GAB bores within the study area, with the only bore screened within the Pilliga Sandstone
273 (273314) (Figure 2). To better constrain GAB groundwater characteristics, we reviewed
274 regional information and used geochemical data from known GAB bores collected by Radke



et al. (2000) and McLean (2003). These data were collected to the northwest of our study area and are used as a range (depending on availability of the original reported data) for the GAB end-member in all future plots and discussions (Supplementary Table 1).

To help in the description of results, we use shallow (< 30 m), intermediate ($30 - 80$ m) and deep (> 80 m) as a rough guide to the origin of the groundwater sample. The chosen depth categories are based on clusters and trends in the ^{14}C analyses. Groundwater samples from similar contemporaneous alluvial-filled valleys in other eastern Australian river valleys show a continuum of geochemical evolution that cannot be explained by separating samples into arbitrary aquifers (such as the aforementioned Narrabri, Gunnedah and Cubbaroo Formations). In such settings, proximity to modern channels and depth are the primary controls on residence time (Cendón et al. 2010; Iverach et al. 2015).

3.2 Geochemical analyses

Groundwater samples from both campaigns were analysed at ANSTO by inductively coupled plasma atomic emission spectroscopy (ICP-AES) for cations and ion chromatography (IC) for anions. The cation and anion analyses were assessed for accuracy by evaluating the charge balance error percentage (CBE%). All samples fell within the acceptable $\pm 5\%$ range, except for samples 25327-1 and 36001-1, which both contained high NH_4^+ concentration that was not part of the initial ion analyses. Samples for $\delta^2\text{H}$ and $\delta^{18}\text{O}$ were analysed using Cavity Ring-Down Spectroscopy (CRDS) on a Picarro L2130-*i* analyser. These values are reported as ‰ deviations from the international standard V-SMOW (Vienna Standard Mean Ocean Water) and results are accurate to $\pm 1\%$ for $\delta^2\text{H}$ and $\pm 0.15\%$ for $\delta^{18}\text{O}$.

The ^{14}C samples were processed and analysed at ANSTO using methods described in Cendón et al. (2014). The ^{14}C activities were measured by accelerator mass spectrometry (AMS) using the ANSTO 2MV tandemron accelerator, STAR (Fink et al. 2004). The ^{14}C results



300 were reported as percent modern carbon (pmc) following groundwater ^{14}C reporting criteria
301 (Mook & van der Plicht 1999; Plummer & Glynn 2013) with an average 1σ error of 0.21 pmc
302 (pmc and pMC values are included in Supplementary Table 3 for completeness).

303 The ^3H samples were analysed at ANSTO. Water samples were distilled and
304 electrolytically enriched prior to analysis by liquid scintillation. The ^3H concentrations were
305 expressed in tritium units (TU) with a combined standard uncertainty of ± 0.03 TU and
306 quantification limit of 0.04 TU. Tritium was measured by counting beta decay in a liquid
307 scintillation counter (LSC). A 10 mL sample aliquot was mixed with the scintillation cocktail
308 that releases a photon when struck by a beta particle. Photomultiplier tubes in the counter
309 convert the photons to electrical pulses that are counted over 51 cycles for 20 minutes.

310 The $^{36}\text{Cl}/\text{Cl}$ and $^{36}\text{Cl}/^{37}\text{Cl}$ ratios were measured by AMS using the ANSTO 6MV SIRIUS
311 Tandem Accelerator (Wilcken et al. 2017). Samples were processed in batches of 10, with
312 each batch containing 1 chemistry blank. The amount of sample used was selected to yield ~
313 5 mg of Cl for analysis without carrier addition. Chloride was recovered from the sample
314 solutions by precipitation of AgCl from hot solution (Stone et al. 1996). This AgCl was re-
315 dissolved in aqueous NH_3 (20-22 wt %, IQ grade, Seastar) to remove sulfur compounds of Ag.
316 Owing to isobaric interference of ^{36}S with ^{36}Cl in the AMS measurements, a saturated
317 $\text{Ba}(\text{NO}_3)_2$ solution (99.999% trace metal basis) was used to precipitate sulfur as BaSO_4 . At
318 least 72 h were allowed for BaSO_4 to settle from a cold solution (4°C) in the dark before
319 removal of the supernatant by pipetting and filtration (0.22 Millex GS). Pure AgCl was re-
320 precipitated by acidifying the $\text{Ag}(\text{NH}_3)_2\text{-Cl}$ solution with 5M nitric acid (IQ Seastar, sub-
321 boiled). Finally, AgCl was recovered, washed twice and dried. It was then pressed into high-
322 purity AgBr (99% trace metal basis, Aldrich) in 6 mm diameter Cu-target holders. AgBr has a
323 much lower sulfur content than Cu. The stable Cl isotopes ^{35}Cl and ^{37}Cl were measured with
324 Faraday cups and ^{36}Cl events were counted with a multi-anode gas ionisation chamber. Gas



(Ar) stripping (for good brightness/low ion straggling) the ions to 5+ charge state in the accelerator terminal suffices for effective ^{36}S interference separation in the ionisation chamber combined with sample-efficient and rapid analysis. Purdue PRIMELab Z93-0005 (nominally 1.20×10^{-12} $^{36}\text{Cl}/\text{Cl}$) was used for normalisation with a secondary standard (nominally 5.0×10^{-13} $^{36}\text{Cl}/\text{Cl}$ (Sharma et al. 1990)) used for monitoring. Background subtraction was done with a linear dependence between ^{36}Cl -rate and interfering ^{36}S -rate. This dependency is established by combining all the blank and test sample measurements and applied to the unknown samples during offline data analysis. This correction factor was typically less than analytical uncertainty of 3-4% bar one sample that had a correction factor of 12% with an analytical uncertainty of 6%.

335

336 4 Results and Discussion

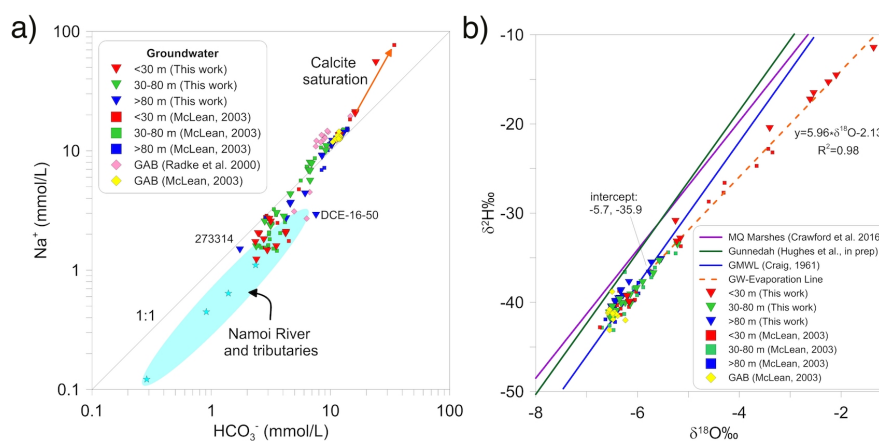
337 4.1 Identification of recharge and mixing between the GAB and the LNA

In the literature, mechanisms of recharge to the LNA are generally agreed upon, with a main surface water recharge component and a minor artesian component (Calf 1978; Merrick 2000; McLean 2003). We observe these two mechanisms in this study as well, however the relative contributions of these two components at any given time, and how this contribution changes over time, are difficult to constrain.

There is an excess of both Na^+ and HCO_3^- in the groundwater of the LNA (Supplementary Table 2), compared to ion ratios expected from local rainfall sources and other shallow groundwater alluvial systems in eastern Australia (Martinez et al. 2017). Their abundance defines the ubiquitous presence of Na- HCO_3 -type groundwater we observe throughout the study area. The Na- HCO_3 ratio in GAB groundwater is generally 1:1 (ppm) (Radke et al. 2000; McLean 2003), which is reinforced by the position of the regional GAB samples in Figure 3a. The Namoi River and other regional streams have lower Na^+ and



350 HCO_3^- concentrations and a lower $\text{Na}^+/\text{HCO}_3^-$ ratio than both the historic GAB data and the
 351 deeper alluvial data collected in this study. Figure 3a shows a mixing line that the alluvial
 352 samples follow, plotting between the end-members of the GAB and the Namoi River. This
 353 suggests that there is an increasing GAB contribution to the alluvial groundwater with depth
 354 and that a continuum of mixing exists between the shallow and deep groundwater within the
 355 LNA. The shallow samples (25220-1 and 30259-1) that are more Na^+ enriched compared to
 356 samples from the GAB have undergone separate evapotranspiration processes and hence have
 357 a concurrent increase in Cl^- . The evapotranspiration process is also shifting the groundwater
 358 composition towards calcite saturation. Both processes contribute to increasing the
 359 $\text{Na}^+/\text{HCO}_3^-$ ratio. The evaporative enrichment is also evident in the concentration of F^- , Cl^-
 360 and the Cl^-/Br^- ratio (Figure 4). Evidence for the CaCO_3 precipitation is found in the calcrete
 361 material on the surface soils, which also occurs in other semi-arid environments due to this
 362 process (Meredith et al. 2016).



363

364 **Figure 3.** a) Na^+ vs HCO_3^- showing the mixing trend that the alluvial samples form between the
 365 Namoi River and samples from the GAB (Radke et al. 2000; McLean 2003). The shaded blue ellipse
 366 represents all river chemistry data available for the Namoi River and tributaries (this work (n=4),
 367 McLean 2003 (n=4), Mawhinney 2011 (n=79)); b) Water stable isotopes in the LNA, showing the two



368 separate mechanisms of recharge; surface water recharge plotting along an evaporation trend line and
369 potential inflow from the GAB clustered with regional samples from the GAB (McLean 2003).

370

371 The $\delta^{18}\text{O}$ and $\delta^2\text{H}$ compositions suggest two mechanisms of recharge to the alluvium
372 (Figure 3b; Supplementary Table 3): artesian discharge and surface water infiltration. The
373 regional GAB samples ($\delta^{18}\text{O}$ and $\delta^2\text{H}$: -6.58‰ to -6.24‰ and -43.1‰ to -38.8‰,
374 respectively (McLean 2003)) plotted within the alluvial groundwater sample range ($\delta^{18}\text{O}$ and
375 $\delta^2\text{H}$: -7‰ to -6‰ and -44‰ to -37‰, respectively). This may suggest a GAB component in
376 the alluvium. A second trend is observed with alluvial groundwater samples ranging from -
377 3.4‰ to -1.4‰ for $\delta^{18}\text{O}$ and -20.5‰ to -11.5‰ for $\delta^2\text{H}$ plotting along an evaporation trend
378 line that suggests good connection and mixing between modern surface water and shallow
379 groundwater.

380 Further hydrochemical evidence for these recharge mechanisms come from assessing
381 the covariation of Na^+ and F^- , both interpreted as primarily derived from groundwater
382 interaction with silicate minerals in this region (Airey et al. 1978; Herczeg et al. 1991;
383 McLean 2003) (Figure 4a). Our alluvial samples fall on the mixing line between samples
384 from the river and nearby tributaries and regional samples from the GAB (Radke et al. 2000),
385 in a similar way to the Na-HCO_3 trend that we observe in Figure 3a. The Cl^-/Br^- ratios in the
386 groundwater also support the mixing interpretation provided by the Na^+ and HCO_3^-
387 concentrations, contrary to the possibility of water rock interactions along the alluvium
388 flowpath (Figure 4b). The Cl/Br ratios in shallow samples connected to the river are
389 consistent with expected ratios in rainfall (Short et al. 2017). The regional GAB samples
390 (Radke et al. 2000) show a Cl^-/Br^- ratio closer to seawater, with our samples from the LNA
391 lying on a mixing trend between the two end-members.

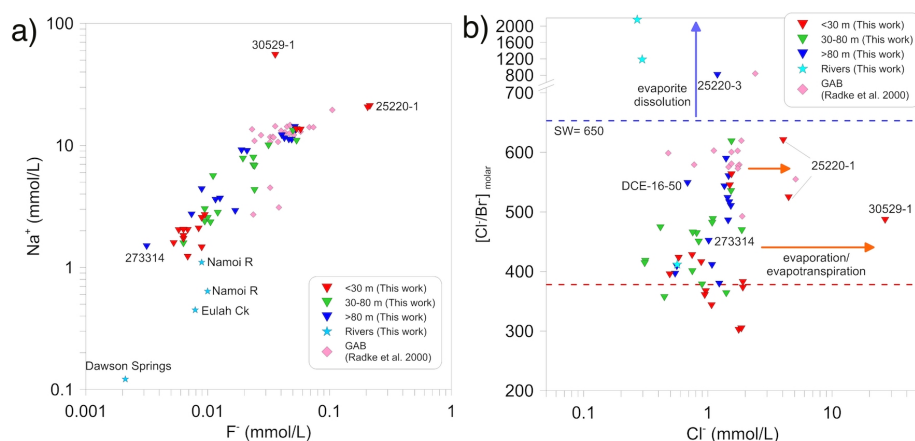


Figure 4. a) Na⁺ vs F⁻ and b) Cl⁻/Br⁻ vs Cl⁻, highlighting the mixing trend between the surface recharge and the GAB that we observe in other geochemical indicators. The red dotted line represents the Cl⁻/Br⁻ ratio for rainfall.

Figure 4a also reveals a deep outlying sample (273314), which was 207 m bgs in total depth (screened 182-195 m bgs), yet plots with the shallow alluvial and river samples. Additionally, many of the geochemical parameters in this sample have a signature similar to river water rather than what would be expected in the GAB 207 m bgs (Supplementary Tables 2 and 3). Figure 2 shows that this sample is situated just above the Napperby Formation. This suggests that this sample originated from surface recharge from the Namoi River (which is in contact with the underlying Digby Formation to the south of the study area), with negligible input from the more Na-HCO₃-rich groundwater in the overlying Pilliga Sandstone. We observe a similar geochemistry in sample 30345-2 (Supplementary Tables 2 and 3), which is situated in the lower part of the LNA in proximity to the alluvial contact with the Napperby Formation (Figure 2). These results suggest the connection between deeper Triassic formations beneath the GAB and the Namoi River, which must be an important consideration in future water balance models of the catchment.



410

411 **4.2 Mixing between groundwaters of varying residence times**

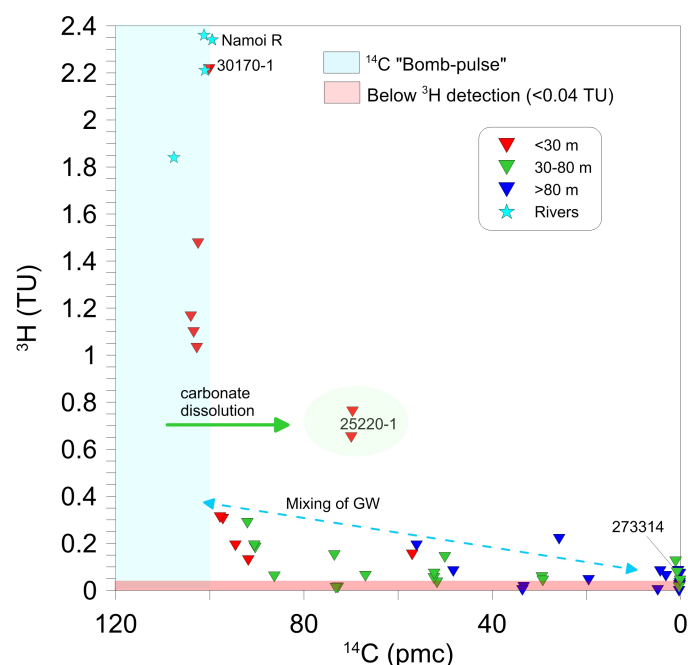
412 Major ion and water stable isotope data suggest that there is mixing of groundwater from the
413 GAB and the LNA. We build upon this interpretation by evaluating the ^3H and ^{14}C contents
414 in the groundwater of the LNA and calculating residence times from ^{36}Cl , to quantify the
415 extent of interaction between the two groundwater sources.

416 Tritium activities vary throughout the study area, with activities generally decreasing
417 with depth and distance from the river channel (Supplementary Table 3). The activities of ^3H
418 in shallow groundwater samples near the main channels show areas with modern recharge.
419 However, despite decreasing activities, ^3H remains relatively prevalent in the deeper part of
420 the system. This indicates the extent of recharge from episodic flooding and shows that
421 surface recharge reaches the deeper LNA (down to ~80 m bgs) relatively quickly (< 70
422 years). In February 1971, the region experienced the second largest flood on record. Pre-
423 flood sampling of deep groundwater (> 70 m bgs) revealed ^3H activities ranging from 7.9 to
424 11.2 TU, in several bores located in the north of our study area (Calf 1978). The same
425 monitoring bores in September 1971 and March 1972 ranged from 16.6 to 20.7 TU, with
426 surface water in the Namoi River ranging from 16.9 to 22.3 TU (Calf 1978). Pre-flooding ^3H
427 activities suggest that modern water was already present in deeper parts of the alluvial aquifer
428 at this time, indicating good connectivity to the surface and that substantial recharge took
429 place during this flood, highlighting the importance of surface water recharge to the LNA. It
430 should be noted that the high ^3H values in the 1970s are a result of atmospheric nuclear bomb
431 testing and can't be compared with present day ^3H values.

432 The prevalence of ^3H throughout the system (indicating groundwater with a residence
433 time of < 70 a) is not consistent with the ^{14}C contents in the groundwater (Supplementary
434 Table 3). The presence of measurable ^3H but negligible ^{14}C (close to 0 pmc) suggests that



435 mixing is occurring between groundwater that is associated with modern recharge processes
 436 in the alluvium and groundwater that is presumably much older as indicated by the ^{14}C
 437 content and may be derived from artesian inflow. Figure 5 shows ^3H activities above the
 438 detection limit in samples with ^{14}C content of almost 0 pmc, suggesting that groundwater
 439 with a very low ^{14}C content is mixing with groundwater with a high ^3H activity. Even though
 440 we see evidence of ^{14}C dilution in localised areas, we also observe mixing between
 441 groundwaters of widely different ^{14}C and ^3H values in the gradient of the samples in Figure 5
 442 (emphasised with a dotted blue line). This gradient would be steeper if there were mixing
 443 between groundwaters closer in residence times (Cartwright et al. 2013). The outlying sample
 444 (25220-1) is interpreted to be undergoing carbonate dissolution as evidenced by calcrete
 445 material present in the surface soils.



446
 447 **Figure 5.** ^3H (TU) vs ^{14}C (pmc). This shows the mixing between groundwater with detectable ^3H
 448 activity and groundwater with very low ^{14}C content (as indicated by the dotted blue line).



449

450 **4.3 Extent of interaction between the GAB and the LNA**

451 The ^3H and ^{14}C values show that there is mixing between groundwater of varying values,
452 however they provide little constraint on the groundwaters with a ^{14}C content of close to 0
453 pmc (ie > 30 ka). This is where chlorine-36 dating can be a useful tracer because it can be
454 used to identify the presence of groundwaters that are much older than the range provided by
455 ^{14}C . It has been found that groundwater in the GAB recharge zone closest to the study area
456 has a $^{36}\text{Cl}/\text{Cl}$ ratio up to ~ 200 ($\times 10^{-15}$) (Radke et al. 2000) with recharge values applied in
457 calculations elsewhere in the GAB of 110 ($\times 10^{-15}$) (Moya et al. 2016). Water from the Namoi
458 River has a $^{36}\text{Cl}/\text{Cl}$ ratio of ~ 420 ($\times 10^{-15}$), possibly affected by thermonuclear ^{36}Cl input from
459 atmospheric bomb testing in the 1950s (Supplementary Table 4). We calculated ^{36}Cl ages
460 from the equations of Bentley et al. (1986), assuming no other sources or sinks besides
461 recharge and natural decay (eqn. 1):

$$462 \quad t = \frac{-1}{\lambda_{36}} \ln \frac{R - R_{se}}{R_0 - R_{se}} \quad (1)$$

463 where $R = ^{36}\text{Cl}/\text{Cl}$ ratio measured in the sample, $R_0 =$ the initial $^{36}\text{Cl}/\text{Cl}$ ratio (meteoric
464 water), and $R_{se} =$ the $^{36}\text{Cl}/\text{Cl}$ ratio under secular equilibrium (in this case the $^{36}\text{Cl}/\text{Cl}$ ratio
465 from the Pilliga Sandstone). We used a R_0 value of 160 ($\times 10^{-15}$), which was an average of 10
466 samples compiled from studies in the Coonamble Embayment and reported in Radke et al.
467 (2000). For R_{se} we used a value of 5.7 ($\times 10^{-15}$), which is appropriate for aquifers dominated
468 by sandstone (this secular equilibrium value can vary according to the dominant lithology).
469 This R_{se} value has been applied to $^{36}\text{Cl}/\text{Cl}$ calculations elsewhere in the GAB (Moya et al.
470 2016).

471 A plot of $^{36}\text{Cl}/\text{Cl}$ vs ^{14}C (pmc) (Figure 6) shows a distinct mixing trend between
472 groundwater with high and very low ^{14}C content. The 2 deep outlying samples (30345-2 and
473 273314; shaded yellow ellipse in Figure 6) display different geochemical characteristics from



the other samples, possibly because of its proximity to the Napperby Formation (Figure 2).
 Figure 6 shows the $^{36}\text{Cl}/\text{Cl}$ value range of GAB recharge, highlighting the alluvial samples
 with values lower than this GAB recharge value. This suggests that these alluvial
 groundwaters are influenced by artesian inflow of very old groundwater. In this case, the
 longest residence time calculated from eqn. 1 is between 700 ka and ~900 ka. Using the two
 extremes of the $^{36}\text{Cl}/\text{Cl}$ range for GAB recharge (100×10^{15} and 200×10^{15}) this calculated
 residence time would be slightly shorter or slightly longer, respectively.

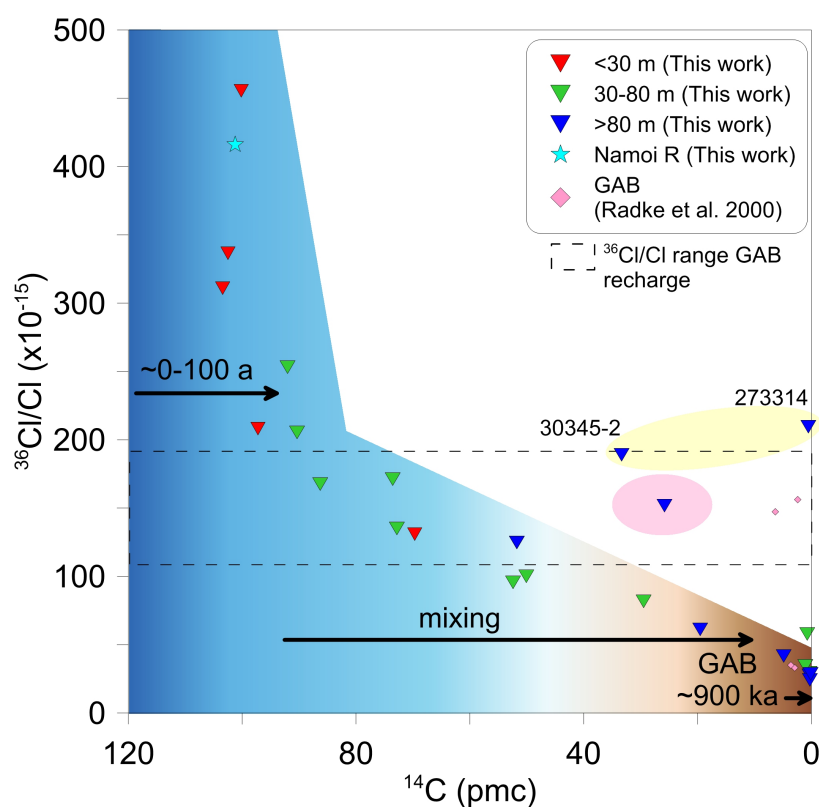
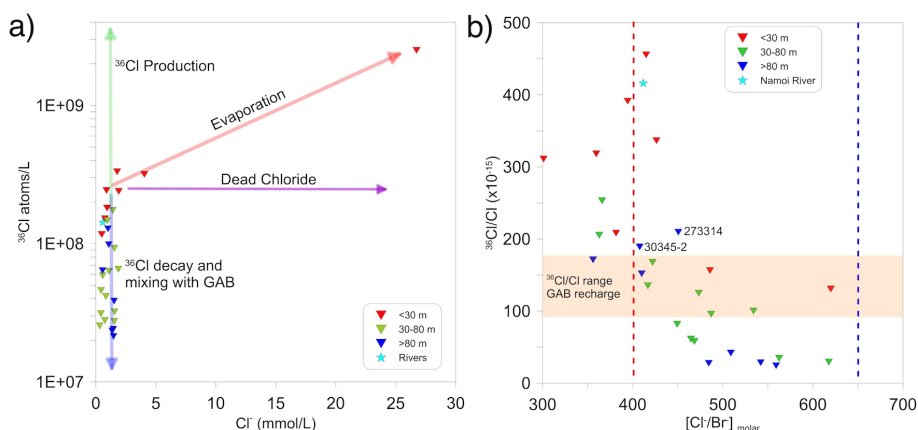


Figure 6. $^{36}\text{Cl}/\text{Cl}$ ($\times 10^{-15}$) vs ^{14}C (pmc). The colour gradient represents the mixing between the two
 major sources: surface water recharge (modern) and the GAB (old). The shaded yellow ellipse
 encompasses the two outliers where the geochemistry is being influenced by proximity to the
 Napperby Formation. The shaded pink ellipse is sample 25327-3 located in the irrigation area.



487 The apparent degree of ^{36}Cl decay we observe in the alluvial groundwater samples is
 488 too large to be explained simply by radioactive decay as indicated by the measurable ^{14}C
 489 content in the same samples. This means that the time needed for the ^{36}Cl to decay as much
 490 as we observe would be well outside the range of ^{14}C dating (> 30 ka) and therefore we
 491 would expect all groundwater samples to have a ^{14}C content of 0 pmc, which we do not
 492 observe. Furthermore, the decrease in ^{36}Cl is unlikely to result from dilution by ^{36}Cl -depleted
 493 sources such as evaporites, as the Cl^- concentrations are similar in most samples (Figure 7a
 494 and b). Therefore, mixing between groundwaters of different residence times is the most
 495 likely explanation for the observed ^{36}Cl signatures.



496 **Figure 7.** a) ^{36}Cl vs Cl^- concentration. The ^{36}Cl production arrow represents in situ ^{36}Cl production as
 497 a result of high U and Th in host rocks; b) $^{36}\text{Cl}/\text{Cl}$ ratio ($\times 10^{-15}$) vs Cl^-/Br^- . The dotted blue line
 498 represents the Cl^-/Br^- ratio in seawater and the dotted red line represents the expected Cl^-/Br^- ratio for
 499 rainfall at Narrabri based on distance from the coast (Short et al. 2017).

501
 502 Our groundwater samples from the deep alluvium display lower $^{36}\text{Cl}/\text{Cl}$ ratios (down to
 503 $24 (\times 10^{-15})$) than those measured in the GAB recharge zone. This indicates that there is very
 504 old groundwater in the deeper LNA (up to 900 ka), and that the mixing that we observe in our



505 geochemical data could be taking place between groundwater with a residence time of less
506 than 70 a (assumed using ^3H) and groundwater with a residence time ~ 900 ka (calculated
507 using ^{36}Cl ; an approximation based on eqn. 1). In the study area, the only source of
508 groundwater with a residence time ~ 900 ka is the GAB.

509 To quantify the extent of interaction between the two groundwater sources, we use the
510 concentration of the conservative chloride ion to determine an approximate percentage of
511 GAB to alluvial groundwater at each sample location. To estimate the local surface
512 infiltration end-member, we used a shallow groundwater sample with a high ^3H activity
513 (sample 30170-1; 2.21 TU). We used the average of all available GAB data as that of GAB
514 inputs. These end-members are mixed in varying proportions to obtain the Cl^- concentration
515 that we observe in all our groundwater samples. In some instances, if the Cl^- concentration in
516 the sample was lower than that in the representative local surface infiltration sample, a 100%
517 LNA contribution is assumed. The representative sample used as the local surface infiltration
518 end-member is evaporated (Figure 3b; Supplementary Table 2) and therefore does not have
519 the lowest Cl^- concentration in the alluvium. If we were to use the sample with the lowest Cl^-
520 concentration as the surface water end-member, we would require a higher percentage of
521 GAB contribution across the study area. Thus, the use of the evaporated sample as our end-
522 member represents a conservative approach to consider overall transport of Cl^- from shallow
523 groundwater.

524 The Cl mixing results provide an approximate mixing threshold with shallower samples
525 generally containing a higher proportion of alluvial groundwater, which diminishes with
526 depth. These mixing proportions show that some deeper samples in the LNA contain up to
527 70% GAB groundwater. Figure 8 presents approximate contours for artesian discharge
528 proportions into the LNA based on the Cl mixing approach. The dotted lines indicate areas



where we have only one sample to inform interpretations, whereas the solid lines connect multiple samples that all displayed similar contributions from the GAB.

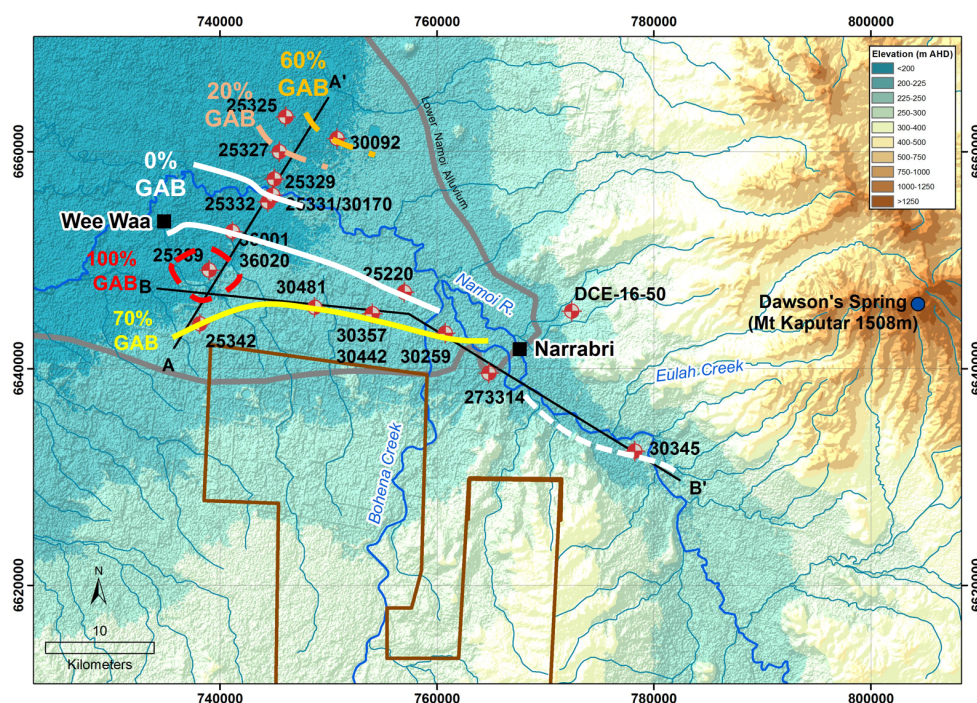


Figure 8. Approximate percentages of GAB contribution to the LNA, calculated from multiple geochemical tracers and major ion data.

Artesian input can be inferred from nested piezometers at locations 30481 and 30259 (Figure 1). At these locations, the monitoring bore slotted in the lower portion of the LNA has a head higher than the monitoring bore slotted in the shallow portion of the LNA, indicative of upward flow. At all other locations artesian contributions cannot be discerned from head data. Comparing Figure 8 to Figure 1 we show that groundwater geochemistry can provide a more accurate evaluation of GAB contribution to the LNA. Multiple geochemical tracers reveal that boreholes in the north and west of the study area may be experiencing much more GAB inflow than has been inferred in catchment water balance models (Merrick



2001; Kelly et al. 2007; CSIRO 2007). This is most evident at sample 25342. It is not immediately apparent from the vertical heads in the hydrograph set at sample 25342 that there is any GAB inflow, yet based on the geochemical tracers this location is 100 % GAB groundwater. The water balance model presented in Merrick (2001) has GAB groundwater contributing 22% of all inflow into the LNA between Narrabri and Wee Waa (Figure 1). From the geochemistry alone it is not possible to make an estimate that can be directly compared to the artesian discharge estimates presented in Merrick (2001). However, it is apparent from the mixing results shown in Figure 8 that a large portion of the study area has an artesian input to the LNA that is greater than 22%. This indicates that it is necessary to consider the geochemistry of the groundwater in conjunction with water balance modelling to constrain estimates of artesian discharge to an alluvial aquifer.

554

555 4.4 Temporal changes in the interaction between the LNA and the GAB

556 The multiple geochemical tracers we have used show substantial artesian discharge to the
557 LNA, which is larger than that currently considered in groundwater models of the region
558 (Merrick 2001; Kelly et al. 2007; CSIRO 2007). Time series sampling constrains how this
559 interaction between the GAB and the LNA changes over time and is important for
560 understanding future artesian contributions to the LNA. We used ^{14}C (pmc) data collected in
561 1978 (Calf), 2003 (McLean), 2010 (ANSTO data) and 2016 (this study) to observe how the
562 ^{14}C content in the groundwater changes over time. Even though dissolved inorganic carbon
563 content and isotopic signature can be affected by processes involving both organic and
564 inorganic carbon sources along its flow path, (which can alter the ^{14}C content) the application
565 of ^{14}C data can still be useful as a tracer when investigating mixing and recharge processes
566 (Meredith et al. 2016). This is especially the case if it is assumed that the processes that can
567 potentially alter the ^{14}C signature do not change over the period where different historical ^{14}C



568 data are compared. Therefore, the historical ^{14}C data, coupled with data from this study could
569 be used to estimate the changes in relative contributions of high ^{14}C contents from recent
570 groundwater recharge from the surface (~ 100 pmc) versus low ^{14}C contents of the GAB
571 groundwater to the LNA. The dataset contains 14 bores from 5 nested sites and is the most
572 comprehensive long-term time-series database for the study area, if not Australia, despite not
573 being complete for all years.

574 Most of the samples displayed relatively consistent ^{14}C values across the years where
575 data were available. However, we observed large changes in ^{14}C content in 5 monitoring
576 bores; 4 showed an increase and 1 showed a decrease (bold text in Table 1). The borehole
577 that displayed a decrease in ^{14}C (30092-2) between 2003 and 2016 suggests that there is an
578 increasing GAB contribution over the time period at this site. Using the Cl^- concentration,
579 this sample displayed 60% GAB contribution (Figure 8), despite the vertical head gradients
580 in the hydrograph showing no evidence of this (Figure 1). The remaining 4 monitoring bores,
581 primarily located deeper in the LNA, have an increase in ^{14}C , suggesting a larger alluvial
582 contribution at these locations over time. At monitoring bore 25332-4, ^{14}C increased between
583 1978 and 2010, then decreased between 2010 and 2016. These locations were in the northern
584 part of the study area where there is extensive pumping for irrigation, suggesting that these
585 changes in the ^{14}C contents are reflecting the extent of pumping occurring and associated
586 surface water recharge with modern carbon versus artesian discharge. Therefore, measuring
587 the ^{14}C in the groundwater at any future time and assessing how this has changed using past
588 data is useful as a preliminary indicator for the current state of the system.

589



Table 1. Changes in ^{14}C content (pmc) in select boreholes in the study area between 1978-2016 (see Figures 1 and 8 for the locations of the bores). The 5 bores in bold text highlight where we observe changes in the ^{14}C content from 1978 to this study. Where available, the time of sampling is included.

Bore	Depth interval (m bgs)	Calf (1978)	McLean (2003)	ANSTO data (summer 2010)	This study (summer 2016)	This study (winter 2016)
25220/1	24.4-30.5	28.15	ND	ND	69.66	69.94
25220/3	97.5-109.7	0.99	ND	0.13	0.17	0.22
25325/2	36.9-38.4	83.63	ND	85.77	86.25	ND
25325/6	67.1-70.1	65.31	ND	66.57	90.37	ND
25332/1	17.7-21	103.61	ND	ND	102.48	ND
25332/2	38.1-41.1	99.19	ND	104.78	ND	ND
25332/3	50.9-55.5	94.70	ND	ND	ND	ND
25332/4	66.8-69.8	49.33	ND	84.12	73.57	ND
25327/1	18.9-21.9	123.36	101.3 (s)	ND	103.43	102.74
25327/2	57.9-60.9	84.16	93.78 (s)	ND	92.05	90.56
25327/3	80.8-83.8	8.48	8.63 (s)	ND	25.79	56.08
30092/1	17.7-20.7	ND	90.51 (w)	ND	ND	ND
30092/2	48.2-49.4	ND	80.06 (w)	72.31	ND	66.92
30092/4	108.2-110	ND	0.19 (w)	0.24	0.3	0.21

4.5 Implications for sustainable groundwater use

The continued sustainable access to groundwater is vital for irrigation, stock and domestic water supplies in the study area. Increased reliance by the irrigation industry on GAB groundwater with high Na^+ concentrations and very long residence times could have negative environmental impacts, such as producing sodic soils, as well as a significant economic impact. The difficulty in accurately constraining how the artesian contribution to the LNA will change over time means consistent monitoring of the groundwater is important for assessing changes to groundwater quality and quantity and the impact that this will have on the irrigation industry in the region. Additionally, the percentage extent of the interaction between the GAB and the LNA (Figure 8), and how this percentage changes over time depending on surface water recharge and increased groundwater extraction, has repercussions for the continued access and management of groundwater in the LNA. In regions where very old groundwater is used, assessments of sustainability must consider changing water quality (for example salinity and the sodium adsorption ratio (SAR)), as well as changes to



608 groundwater heads throughout the system, especially in recharge areas. Our results indicate
609 that the head in the GAB needs to be carefully monitored and recharge areas in the alluvium
610 and adjacent rock formations preserved.

611

612 **5 Conclusion**

613 We have used multiple geochemical tracers to show that artesian discharge to a shallow
614 alluvial aquifer is higher than previously derived from water balance models in the literature
615 (Merrick 2001; CSIRO 2007). This finding is important when considering the sustainable use
616 of connected alluvial and artesian systems. We have also provided a percentage estimate of
617 GAB groundwater in each sample collected in the LNA using the concentration of Cl in the
618 groundwater, showing that in some locations the ‘alluvial’ sample is comprised of up to 70%
619 GAB groundwater. Ongoing and increasing artesian inflow into the LNA will change the
620 chemistry of the groundwater used for irrigation, which may have potential impacts on crop
621 yield and soil health.

622 Isotopic tracers (^3H , ^{14}C , and ^{36}Cl) indicate that there is substantial mixing between two
623 groundwaters of very different residence times (< 70 a and ~ 900 ka). This suggests
624 interaction between modern surface recharge through the shallow LNA and variable artesian
625 inflow at depth, dependent on where the sample is located in the system. We used past ^{14}C
626 data (1978, 2003, 2010), along with data from this study to show that there has been an
627 increase in ^{14}C in the groundwater in some locations of the LNA in the last ~ 40 years. This
628 suggests a greater contribution from modern river and flood recharge in locations proximal to
629 the Namoi River since 1978, which could be induced by nearby groundwater abstraction for
630 irrigation. In contrast, a sample farther from the river has displayed a steady decrease in ^{14}C
631 content since 1978. How these trends change geographically throughout the system, and how
632 they will behave in the future are difficult to constrain without continuous monitoring.



Recharge inputs to the LNA from the GAB were previously considered less than 22% (Merrick 2001; CSIRO 2007). However, we have shown that GAB discharge is occurring in locations where inflow is not apparent from the nested hydrograph data. This highlights the need to apply multiple groundwater investigation techniques (including flow modelling, hydrograph analysis, geophysics, and geochemistry) when inferring artesian discharge to an alluvial aquifer. We have shown that a multi-tracer geochemical approach is required to better determine artesian contributions to the alluvial aquifer and must be considered in constraining future models of the study system and elsewhere.

641

642 **Acknowledgements**

This research was funded by the Cotton Research and Development Corporation (CRDC). Charlotte Iverach was supported by scholarships from the Australian Government, ANSTO and CRDC. ANSTO support and analytical staff are thanked for their continuous efforts (Chris Dimovski, Henri Wong, Robert Chisari, Vladimir Levchenko, Krista Simon, Alan Williams, Simon Varley). The authors also thank Dr. Lisa Williams for editing and proofreading the manuscript.

649

650 **Author contributions**

Experimental conceptualisation and design was carried out by D.I.C & B.F.J.K. Fieldwork was conducted by C.P.I., D.I.C., S.I.H. & B.F.J.K. Additional data was contributed by K.T.M. Geochemical analyses were conducted by C.P.I., D.I.C. & K.M.W. The manuscript was written by C.P.I with input from all authors.

655

656 **Competing Interests**

The authors declare that they have no conflict of interest.

657



658

659 **6 References**

660 Abid, K., Dulinski, M., Ammar, F.H., Rozanski, K. & Zouari, K. Deciphering interaction of regional aquifers in
661 Southern Tunisia using hydrochemistry and isotopic tools. *Appl. Geochem.* **27**, 44-55, 2012.

662

663 Acworth, R.I., Timms, W.A., Kelly, B.F.J., McGeeney, D.E., Ralph, T.J., Larkin, Z.T. & Rau, G.C. Late
664 Cenozoic paleovalley fill sequence from the Southern Liverpool Plains, New South Wales – implications for
665 groundwater resource evaluation. *Aus. J. Earth. Sci.* **62(6)**, 657-680, (2015).

666

667 Airey, P.L., Calf, G.E., Campbell, B.L., Habermehl, M.A., Hartley, P.E., & Roman, D., 1979. Aspects of the
668 isotope hydrology of the Great Artesian Basin, Australia. In: *Isotope Hydrology 1978*, 1, P. 205–219.
669 Proceedings International Symposium on Isotope Hydrology - International Atomic Energy Agency and United
670 Nations Educational, Scientific and Cultural Organisation, Neuherberg, Fed. Rep. Germany, 19–23 June
671 1978. International Atomic Energy Agency, Vienna, 1979.

672

673 Amiri, V., Nakhaei, M., Lak, R. & Kholghi, M. Geophysical, isotopic, and hydrogeochemical tools to identify
674 potential impacts on coastal groundwater resources from Urmia hypersaline Lake, NW Iran. *Environ. Sci. Poll.*
675 *Res.* **23(16)**, 16738-16760, 2016.

676

677 Anderson, M.P. & Woessner, W.W. *Applied Groundwater Modelling: Simulation of Flow and Advective*
678 *Transport*. Academic Press. ISBN: 0-12-059485-4, 1992.

679

680 Andrews, J. N. & J.-C. Fontes, Comment on chlorine 36 dating of very old groundwater, 3, Further results on
681 the Great Artesian Basin, Australia by T. Torgersen et al., *Water Resour. Res.*, **29**, 1871–1874, 1993.

682

683 Barnett B, Townley LR, Post V, Evans RE, Hunt RJ, Peeters L, Richardson S, Werner AD, Knapton A and
684 Boronkay A. Australian groundwater modelling guidelines, Waterlines report, National Water Commission,
685 Canberra, 2012.

686

687 Bentley, H.W., Phillips, F.M., Davis, S.N., Habermehl, M.A., Airey, P.L., Calf, G.E., Elmore, D., Gove, H.E.
688 Torgersen, T. Chlorine 36 dating of very old groundwater. 1. The Great Artesian Basin, Australia. *Water*
689 *Resour. Res.* **22(13)**, 1986.

690

691 Beven, K. *Environmental Modelling: An Uncertain Future?* Routledge, ISBN-13: 978-0415457590
692 ISBN-10: 0415457599, 2009.

693

694 Calf, G.E. An investigation of recharge to the Namoi Valley aquifers using environmental isotopes. *Aust. J. Soil*
695 *Res.* **16**, 197-207, 1978.

696



- 697 Cartwright, I., Weaver, T., Cendón, D.I. & Swane, I. Environmental isotopes as indicators of inter-aquifer
698 mixing, Wimmera region, Murray Basin, Southeast Australia. *Chem. Geol.* **277**, 214-226, 2010.
699
- 700 Cartwright, I., Fifield, L.K. & Morgenstern, U. Using ^3H and ^{14}C to constrain the degree of closed-system
701 dissolution of calcite in groundwater. *Appl. Geochem.* **32**, 118-128, 2013.
702
- 703 Cendón, D.I., Larsen, J.R., Jones, B.G., Nanson, G.C., Rickleman, D., Hankin, S.I., Pyeyo, J.J. & Maroulis, J.
704 Freshwater recharge into a shallow saline groundwater system, Cooper Creek floodplain, Queensland, Australia.
705 *J. Hydrol.* **392** (3-4), 150-163, 2010.
706
- 707 Cendón, D.I., Hankin, S.I., Williams, J.P., Van der ley, M., Peterson, M., Hughes, C.E., Meredith, K., Graham,
708 I.T., Hollins, S.E., Levchenko, V. & Chisan, R. Groundwater residence time in a dissected and weathered
709 sandstone plateau: Kulnura-Mangrove Mountain aquifer, NSW, Australia. *Aus. J. Earth Sci.* **61**(3), 475-499,
710 2014.
711
- 712 Chen, Z., Nie, Z., Zhang, G., Wan, L. & Shen, J. Environmental isotopic study on the recharge and residence
713 time of groundwater in the Heihe River Basin, northwestern China. *Hydrogeol. J.* **14**(8), 1635-1651, 2006.
714
- 715 Clark, I.D. & Fritz, P. Age Dating Old Groundwater in Environmental Isotopes in Hydrogeology. CRC Press,
716 USA, 1997.
717
- 718 Costelloe, J.F., Irvine, E.C., Weestern, A.W. & Tyler, M. Identifying fluvial recharge and artesian upwards
719 leakage contributions to arid zone shallow, unconfined groundwater. *Chem. Geol.* **326-327**, 189-200, 2012.
720
- 721 CSIRO. Water availability in the Namoi. A report to the Australian Government from the CSIRO Murray-
722 Darling Basin Sustainable Yields Project. CSIRO, Australia. 154pp., 2007.
723
- 724 Currell, M.J., Werner, A.D., McGrath, C., Webb, J.A. & Berkman, M. Problems with the application of
725 hydrogeological science to regulation of Australian mining projects: Carmichael Mine and Doongmabulla
726 Springs. *J. Hydrol.* **548**, 674-682, 2017.
727
- 728 Dawes, W.R., Gilfedder, M., Walker, G.R. & Evans, W.R. Biophysical modelling of catchment-scale surface
729 water and groundwater response to land-use change. *Math. Comp. Sim.* **64** (1), 3-12, 2004.
730
- 731 Department of Primary Industries (DPI) Water. NSW Government. *Namoi Alluvium Water Resource Plan*
732 *(GW14)*, *Status and Issues Paper*, available at:
733 [http://www.water.nsw.gov.au/__data/assets/pdf_file/0020/701732/Status-and-Issues-Paper-Namoi-GW-](http://www.water.nsw.gov.au/__data/assets/pdf_file/0020/701732/Status-and-Issues-Paper-Namoi-GW-WRP.pdf)
734 *WRP.pdf*, 2017.
735



- 736 Duvert, C., Stewart, M.K., Cendón, D.I. and Raiber, M. Time series of tritium, stable isotopes and chloride
737 reveal short-term variations in groundwater contribution to a stream. *Hydrol. Earth Syst. Sci.* **20**, 257-277, 2016.
738
- 739 Fink, D., Hotchkis, M., Hua, Q., Jacobsen, G., Smith, A.M., Zoppi, U., Child, D., Mifsud, C., van der Gaast, H.,
740 Williams, A. & Williams, M. The ANTARES AMS facility at ANSTO. *Nuc. Instr. Meth. Phys. Res. Sect. B:*
741 *Beam Interac. Mat. Atoms* **223-224**, 109-115, 2004.
742
- 743 Gardner, W.P., Harrington, G.A. & Smerdon, B.D. Using excess ^4He to quantify variability in aquitard leakage.
744 *J. Hydrol.* **468-469**, 63-75, 2012.
745
- 746 Giambastiani, B.M.S., McCallum, A.M., Andersen, M.S., Kelly, B.F.J. & Acworth, R.I. Understanding
747 groundwater processes by representing aquifer heterogeneity in the Maules Creek Catchment, Namoi Valley
748 (New South Wales, Australia), *Hydrogeol. J.* **20(6)**, 1027-1044, 2012.
749
- 750 Herczeg, A.L., Torgersen, T., Chivas, A.R. & Havermehl, M.A. Geochemistry of ground waters from the Great
751 Artesian Basin, Australia. *J. Hydrol.* **126**, 225-245, 1991.
752
- 753 Hocking, M. & Kelly, B.F.J. Groundwater recharge and time lag measurement through Vertosols using impulse
754 response functions. *J. Hydrol.* **535**, 22-35, 2016.
755
- 756 Iverach, C.P., Cendón, D.I., Hankin, S.I., Lowry, D., Fisher, R.E., France, J.L., Baker, A. & Kelly, B.F.J.
757 Assessing connectivity between an overlying aquifer and a coals seam gas resource using methane isotopes,
758 dissolved organic carbon and tritium. *Sci. Rep.* **5**, 1-11, 2015.
759
- 760 Kalaitzis, P. & Jamieson, M. Draft Status Report for the Alluvial Groundwater Resources of the Lower Namoi
761 Valley NSW. Land and Water Conservation Groundwater Unit Barwon Region, 121pp., 2000.
762
- 763 Kelly, B.F.J., Merrick, N., Dent, B., Milne-Home, W. & Yates, D. Groundwater Knowledge and Gaps in the
764 Namoi Catchment Management Area. Cotton Catchment Communities CRC, University of Technology, Sydney
765 – National Centre for Groundwater Management Report, NCGM 2007/1, 70pp., 2007.
766
- 767 Kelly, B.F.J., Timms, W.A., Andersen, M.S., McCallum, A.M., Blakers, R.S., Smith, R., Rau, G.C., Badenhop,
768 A., Ludowici, K. & Acworth, R.I. Aquifer heterogeneity and response time: the challenge for groundwater
769 management. *Crop & Past. Sci.* **64**, 1141-1154, 2013.
770
- 771 Kelly, B.F.J., Timms, W., Ralph, T.J., Giambastiani, B.M.S., Communian, A., McCallum, A.M., Andersen,
772 M.S., Blakers, R.S., Acworth, R.I. & Baker, A. A reassessment of the Lower Namoi Catchment aquifer
773 architecture and hydraulic connectivity with reference to climate drivers. *Aus. J. Earth Sci.* **61**, 501-511, 2014.
774



- 775 Lower Namoi Groundwater, NSW Government Department of Water and Energy, DWE_08_011, 2008,
776 http://www.water.nsw.gov.au/__data/assets/pdf_file/0005/548699/wsp_namoi_gw_info_sheet.pdf
777
- 778 Love, A.J., Herczeg, A.L., Sampson, L., Cresswell, R.G., & Fifield, L.K. Sources of chloride and implications
779 for ^{36}Cl dating of old groundwater, southwestern Great Artesian Basin, Australia, *Water Resour. Res.* **36**, 1561-
780 1574, 2000.
- 781
- 782 Martin, H.A. Cenozoic climatic change and the development of the arid vegetation in Australia. *J. Arid Environ.*
783 **66(3)**, 533-563, 2006.
- 784
- 785 Martinez, J.L., Raiber, M. & Cendón, D.I. Using 3D geological modelling and geochemical mixing models to
786 characterise alluvial aquifer recharge sources in the upper Condamine River catchment, Queensland, Australia.
787 *Sci. Tot. Environ.* **574**, 1-18, 2017.
- 788
- 789 Mawhinney, W. *Namoi Water Quality Project 2002-2007 – Final report*, NSW Office of Water, Sydney, 39 pp,
790 2011. Available at: <http://pandora.nla.gov.au/pan/126486/20110413-1101/namoiwater.pdf>
791
- 792 McLean, W.A. *Hydrogeochemical evolution and variability in a stressed alluvial aquifer system: Lower Namoi*
793 *River catchment, NSW*. PhD thesis, University of New South Wales, Sydney (unpublished), 2003.
- 794
- 795 Meredith, K.T., Han, L.F., Hollins, S.E. Cendón, D.I., Jacobsen, G.E. & Baker, A. Evolution of chemical and
796 isotopic composition of inorganic carbon in a complex semi-arid zone environment Consequences for
797 groundwater dating using radiocarbon. *Geochim. et Cosmochim. Acta* **188**, 352-367, 2016.
- 798
- 799 Merrick, N.P. “Lower Namoi Valley Groundwater Model”, *Heritage Computing Report for Department of*
800 *Water Resources*, New South Wales, 1989.
- 801
- 802 Merrick, N.P. “Lower Namoi Groundwater Flow Model: Conversion to PMWIN Software.” *Insearch Limited*
803 *Report for Department of Land and Water Conservation*, Project No. C98/44/001, September 1998, 56p, 1998a.
- 804
- 805 Merrick, N.P. “Lower Namoi Groundwater Flow Model: Calibration 1987-1994”, *Insearch Limited Report for*
806 *Department of Land and Water Conservation*, Project No. C94/44/005, December 1998, 98p, 1998b.
- 807
- 808 Merrick, N.P. “Lower Namoi Groundwater Flow Model: Scenario Modelling 1994-1997”, *Insearch Limited*
809 *Report for Department of Land and Water Conservation*, Project No. C94/44/005/a, December 1998, 37p,
810 1998c.
- 811
- 812 Merrick, N.P. “Lower Namoi Groundwater Budgets: Simulation 1980-1994”, *Insearch Limited Report for*
813 *Department of Land and Water Conservation (Tamworth)*, Project No. C99/44/008, April 1999, 72p, 1999.
- 814



- 815 Merrick, N.P. "Lower Namoi Groundwater Flow Model: Hydrographic Verification 1980-1994 and
816 Conceptualisation Scenarios", *Insearch Limited Report for Department of Land and Water Conservation*,
817 Project No. C99/44/001, January 2000, 107p, 2000.
- 818
- 819 Merrick, N. P. "Report on Lower Namoi Groundwater Flow Model: Calibration 1980-1998." *Insearch Limited*
820 *Report for Department of Land and Water Conservation. Project C99/44*, 2001.
- 821
- 822 Mook & van der Plicht. Reporting 14C activities and concentrations. *Radiocarbon* **41**, 227-239, 1999.
- 823
- 824 Moya, C.E., Raiber, M., Taulis, M. and Cox, M.E. Using environmental isotopes and dissolved methane
825 concentrations to constrain hydrochemical processes and inter-aquifer mixing in the Galilee and Eromanga
826 Basins, Great Artesian Basin, Australia. *J. Hydrol.* **539**, 304-318, 2016.
- 827
- 828 Nishiizumi, K. 10Be, 26Al, 36Cl, and 41Ca AMS standards: Abstract O16-1. In 9th Conference on Accelerator
829 Mass Spectrometry, page 130, 2002.
- 830
- 831 NSW Pinneena Groundwater Database, NSW Government DPI Water, available at:
832 <http://allwaterdata.water.nsw.gov.au/water.stm>, (last access: 19 May 2017), 2017.
- 833
- 834 Plummer & Glynn. Radiocarbon dating in groundwater systems. In: Isotope methods for dating old
835 groundwater: — Vienna : International Atomic Energy Agency, 2013. Pp. 33-89, STI/PUB/1587, 2013.
- 836
- 837 Powell, J. & Scott, F. A representative irrigation farming system in the Lower Namoi Valley of NSW: an
838 economic analysis. Economic Research Report No. 46, Industry and Investment NSW, 63pp., 2011.
- 839
- 840 Price, G. & Bellis, L. Namoi Catchment Water Study Independent Report Final Study Report. Schlumberger
841 Water Services (Australia) Pty Ltd, 50371/P4-R2 FINAL, 129pp., 2012.
- 842
- 843 Puls, R.W. & Barcelona, M.J. Low-flow (minimal drawdown) groundwater sampling procedures. EPA/540/S-
844 95/504, 10pp., 1996.
- 845
- 846 Radke, B.M., Ferguson, J., Cresswell, R.G., Ransley, T.R. & Habermehl, M.A. Hydrochemistry and implied
847 hydrodynamics of the Cadna-owie-Hooray Aquifer Great Artesian Basin. *Bureau of Rural Sciences, Canberra*,
848 2000.
- 849
- 850 Raiber, M., Webb, J.A., Cendón, D.I., White, P.A. & Jacobsen, G.E. Environmental isotopes meet 3D
851 geological modelling: Conceptualising recharge and structurally-controlled aquifer connectivity in the basalt
852 plains of south-western Victoria, Australia. *J. Hydrol.* **527**, 262-280, 2015.
- 853



- 854 Rawling, G.C. & Newton, B.T. Quantity and location of groundwater recharge in the Sacramento Mountains,
855 south-central New Mexico (USA), and their relation to the adjacent Roswell Artesian Basin. *Hydrogeol. J.*
856 **24(4)**, 757-786, 2016.
- 857
- 858 Reilly T.E. and Harbaugh A.W. Guidelines for Evaluating Ground-Water Flow Models, USGS Scientific
859 Investigations Report 2004-5038, available at: <https://pubs.usgs.gov/sir/2004/5038/PDF.htm>, 2004.
- 860
- 861 Robertson, W.D. & Cherry, J.A. Tritium as an indicator of recharge and dispersion in a groundwater system in
862 Central Ontario. *Water Resour. Res.* **25(6)**, 1097-1109, 1989.
- 863
- 864 “Drilling Methods Bring Spectacular Yield Increases.” Rural Forum for Applied Research in North Western
865 Courier [Narrabri] 11 Dec. 1967: 2. Print.
- 866
- 867 Salameh, E. & Tarawneh, A. Assessing the impacts of uncontrolled artesian flows on the management of
868 groundwater resources in the Jordan Valley. *Environ. Earth Sci.* **76**, 2017.
- 869
- 870 Scanlon, B.R., Healy, R.W. & Cook, P.G. Choosing appropriate techniques for quantifying groundwater
871 recharge. *Hydrogeol. J.* **10 (1)**, 18-39, 2002.
- 872
- 873 Schilling, K.E., Jacobsen, P.J., Libra, R.D., Gannon, J.M., Langel, R.J. & Peate, D.W. Estimating groundwater
874 age in the Cambrian-Ordovician aquifer in Iowa: implications for biofuel production and other water uses.
875 *Environ. Earth Sci.* **76(2)**, 2016.
- 876
- 877 Sharma, P., Kuhik, P.W., Fehn, U., Gove, H.E., Nishiizumi, K. & Elmore, D. *Nucl. Instr. Meth. B.* **52**, 410-415,
878 1990.
- 879
- 880 Short, M.A., de Caritat, P. & McPhail, D.C. Continental-scale variation in chloride/bromide ratios of wet
881 deposition. *Sci. Tot. Environ.* **574**, 1533-1543, 2017.
- 882
- 883 Stone, J.O., Allan, G.L., Fifield, L.K., et al. Cosmogenic chlorine-36 from calcium spallation. *Geochim. et*
884 *Cosmochim. Acta* **60**:679–692, 1996.
- 885
- 886 Smithson, A. *Lower Namoi Groundwater Source: Groundwater Management Area 001 Groundwater Status*
887 *Report 2008*, NSW Department of Water and Energy, Sydney, 2009.
- 888
- 889 Tadros, N.Z. The Gunedah Basin, New South Wales. Vol. 12. *Department of Mineral Resources, Coal and*
890 *Petroleum Geology Branch*, 1993.
- 891



- 892 Torgersen, T., Habermehl, M.A., Phillips, F.M., Elmore, D., Kubik, P., Jones, G.B., Hemmick, T. & Gove, H.E.
893 Chlorine 36 Dating of Very Old Groundwater: 3. Further studies in the Great Artesian Basin, Australia. *Water*
894 *Resour. Res.* **27(12)**, 3201-3213, 1991.
- 895
- 896 Tosaki, Y., Tase, N., Massmann, G., Nagashima, Y., eki, R., Takahashi, T., Sasa, K., Sueki, K., Matsuhiro, T.,
897 Miura, T. & Bessho, K. Application of ^{36}Cl as a dating tool for modern groundwater. *Nuc. Instr. Methods in*
898 *Phys. Res. Sect. B: Beam Interact. with Mat. and Atoms.* **259(1)**, 479-485, 2007.
- 899
- 900 Wilcken, K.M., Fink, D., Hotchkis, M.A.C., Garton, D., Button, D., Mann, M., Kitchen, R., Hauser, T. &
901 O'Connor, A. Accelerator Mass Spectrometry on SIRIUS: New 6 MV spectrometer at ANSTO, *Nucl. Inst. &*
902 *Meth. in Phys. Res. B* xxx, xxx-xxx <http://dx.doi.org/10.1016/j.nimb.2017.01.003>, 2017.
- 903 Williams, R.M., Merrick, N.P. & Ross, J.B. Natural and induced recharge in the Lower Namoi Valley, New
904 South Wales in Sharma, M.L. (ed.) *Groundwater Recharge*, Proceedings of the Symposium on Groundwater
905 Recharge, 239-253, 1989.
- 906 Zhang, L., Walker, G.R. & Dawes, W.R. Water balance modelling: concepts and applications. In. *Regional*
907 *Water and Soil Assessment for Managing Sustainable Agriculture in China and Australia*. ACIAR Monograph
908 No. 84, 31-47, 2002.
- 909

910 **List of Figures**

- 911 **Figure 1.** Map of the study area and sample locations, along with the location of the study
912 area in Australia. Accompanying hydrographs show the groundwater level response in
913 different piezometers throughout the study area (groundwater level data provided by BOM
914 2017). The different colours in the hydrographs represent the different monitoring bores in
915 the nested set. The bottom of the slotted interval for each bore is shown in the key. The x-axis
916 in each hydrograph is the year (1970-2010) and the y-axis is depth (between 0 and 40 m bgs).
917 The two locations with red text highlight areas where the hydrograph heads show clear GAB
918 contribution. The remaining locations show no apparent GAB contribution to the LNA based
919 on the hydrograph data.
- 920 **Figure 2.** Two cross sections through the study area, showing the location and depth of the
921 samples in the alluvium and their proximity to formations of the GAB. Contacts obtained



922 from gas wells Nyora-1, Culgoora-1 and Turrawan-2, coinciding with our cross sections, are
923 added. Their locations are displayed on the map.

924 **Figure 3.** a) Na^+ vs HCO_3^- showing the mixing trend that the alluvial samples form between
925 the Namoi River and samples from the GAB (Radke et al. 2000; McLean 2003). The shaded
926 blue ellipse represents all river chemistry data available for the Namoi River and tributaries
927 (this work ($n=4$), McLean 2003 ($n=4$), Mawhinney 2011 ($n=79$)); b) Water stable isotopes in
928 the LNA, showing the two separate mechanisms of recharge; surface water recharge plotting
929 along an evaporation trend line and potential inflow from the GAB clustered with regional
930 samples from the GAB (McLean 2003).

931 **Figure 4.** a) Na^+ vs F^- and b) Cl^-/Br^- vs Cl^- , highlighting the mixing trend between the surface
932 recharge and the GAB that we observe in other geochemical indicators. The red dotted line
933 represents the Cl^-/Br^- ratio for rainfall.

934 **Figure 5.** ^3H (TU) vs ^{14}C (pmc). This shows the mixing between groundwater with detectable
935 ^3H activity and groundwater with very low ^{14}C content (as indicated by the dotted blue line).

936 **Figure 6.** $^{36}\text{Cl}/\text{Cl}$ ($\times 10^{-15}$) vs ^{14}C (pmc). The colour gradient represents the mixing between
937 the two major sources: surface water recharge (modern) and the GAB (old). The shaded
938 yellow ellipse encompasses the two outliers where the geochemistry is being influenced by
939 proximity to the Napperby Formation. The shaded pink ellipse is sample 25327-3 located in
940 the irrigation area.

941 **Figure 7.** a) ^{36}Cl vs Cl^- concentration. The ^{36}Cl production arrow represents in situ ^{36}Cl
942 production as a result of high U and Th in host rocks; b) $^{36}\text{Cl}/\text{Cl}$ ratio ($\times 10^{-15}$) vs Cl^-/Br^- . The
943 dotted blue line represents the Cl^-/Br^- ratio in seawater and the dotted red line represents the
944 expected Cl^-/Br^- ratio for rainfall at Narrabri based on distance from the coast (Short et al.
945 2017).



946 **Figure 8.** Approximate percentages of GAB contribution to the LNA, calculated from
947 multiple geochemical tracers and major ion data.
948